



University
of Glasgow

Chen, Y. and Cartmell, M.P. (2009) *Hybrid sliding mode control for motorised space tether spin-up when coupled with axial oscillation*. In: *Advanced Problems in Mechanics: Russian Academy of Sciences*, 30 June - 5 July 2009, St Petersburg, Russia.

<http://eprints.gla.ac.uk/30520/>

Deposited on: 23 June 2010

Hybrid Sliding Mode Control for Motorised Space Tether Spin-up when Coupled with Axial Oscillation

Yi Chen* , Matthew P. Cartmell**

yichen@mech.gla.ac.uk matthewc@mech.gla.ac.uk

Abstract

A specialised hybrid controller is applied for the control of motorised space tether spin-up coupled with an axial oscillation phenomenon. A six degree of freedom dynamic model of a motorised momentum exchange tether is used as the basis for interplanetary payload exchange in the context of control. The tether comprises a symmetrical double payload configuration, with an outrigger counter inertia and massive central facility. It is shown that including axial elasticity permits an enhanced level of performance prediction accuracy and a useful departure from the usual rigid body representations, particularly for accurate payload positioning at strategic points. A simulation with a given initial condition data has been devised in a connecting programme between control code written in MATLAB and dynamics simulation code constructed within MATHEMATICA. It is shown that there is an enhanced level of spin-up control for the six degree of freedom motorised momentum exchange tether system using the specialised hybrid controller.

1 Introduction

The concept of the motorised momentum exchange tether (MMET) was first proposed by Cartmell [1], and its modelling and conceptual design were developed further, in particular modelling of the MMET as a rigid body by Ziegler and Cartmell [2], and modelling of the MMET with axial elasticity by Chen and Cartmell [3]. A conceptual schematic of the MMET system with axial elasticity included is shown in Figure 1. The system is composed of the following parts: a pair of braided propulsion tether tube sub-spans, a corresponding pair of braided outrigger tether tube sub-spans, the launcher motor mass within the rotor, and the launcher motor mass within stator, the outrigger masses, and the two payload masses. The MMET is excited by means of a motor, and the model uses angular generalised co-ordinates to represent spin and tilt, together with an angular

co-ordinate for circular orbital motion. Another angular co-ordinate defines backspin of the propulsion motor's stator components. The payload masses are fitted to each end of the tether sub-spans, and the system orbits a source of gravity in space, in this case, the Earth. The use of a tether means that all constituent parts of the system have the same angular velocity as the overall centre of mass (COM). As implied in Figures 1 and 2, the symmetrical double-ended motorised spinning tether can be applied as an orbital transfer system, in order to exploit momentum exchange for propelling and transferring payloads in space.

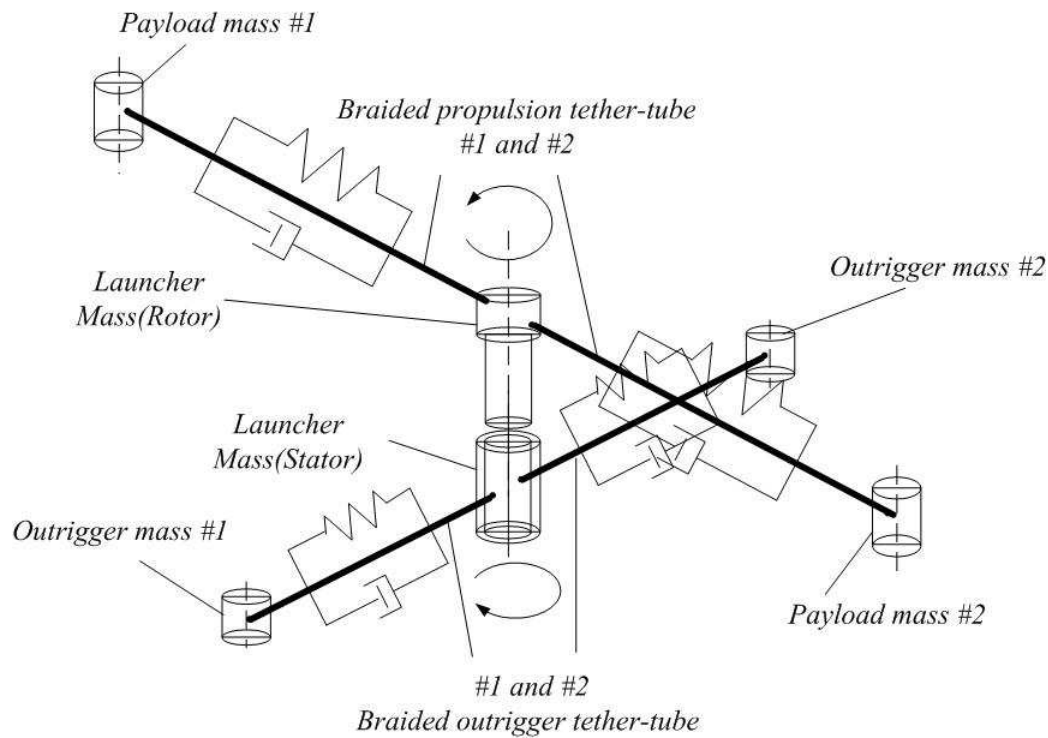


Figure 1: Conceptual Schematic of the Motorised Momentum Exchange Tether with Axial Elasticity

It has been well recognized that fuzzy logic control (FLC) is an effective and potentially robust control method for various diverse applications. The FLC rule-base is generally based on practical human experience, however, the intrinsic linguistic format expression required to construct the FLC rule base makes it difficult to guarantee the stability and robustness of the control system [4].

Variable structure control (VSC) with sliding mode control was introduced in the early 1950s by Emelyanov and subsequently published in the 1960s [5], and then further developed by several other researchers [6][7]. Sliding mode control (SMC) is recognised as a robust and efficient control method for complex, high order, nonlinear dynamical systems. The major advantage of sliding mode control is its low sensitivity to a system's parameter changes under various uncertainty conditions. Another advantage is that it can decouple system motion into independent partial components of lower dimension, which reduces the complexity of the system control and feedback design. However, a major drawback of traditional SMC is a propensity for chattering, which is generally disadvantageous within control systems.

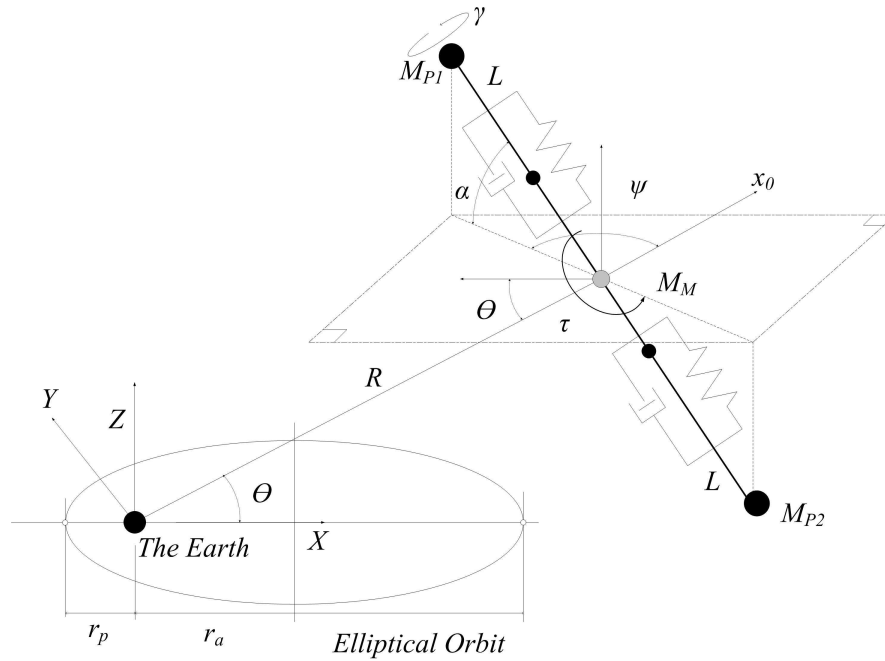


Figure 2: Modelling of the Motorised Momentum Exchange Tether with Axial Elasticity

In recent years, a lot of literature has been generated in the area of fuzzy sliding mode control (FSMC), and this has also covered the chattering phenomenon. The involvement of FLC in the design of a FSMC based controller can be harnessed to help to avoid the chattering problem. The smooth control feature of fuzzy logic can be helpful in overcoming the disadvantages of chattering. This is why it can be useful to merge FLC with SMC to create the FSMC hybrid [8][9][10][11][12][13], and the hybrid fuzzy sliding mode control is defined as F α SMC [14], with a skyhook surface (SkyhookSMC) is applied here to control the tether sub-span length for spin-up control of the MMET system.

2 Six degree of freedom MMET Model

A six degree of freedom non-planar tether model, which includes an axial elasticity coordinate and a solid rolling coordinate, is proposed as an interim model of moderate accuracy for the MMET 6-DOF system, as shown in Figure 2. This discretised MMET system comprises a symmetrical and cylindrical double payload configuration, a cylindrical motor facility, and two axially flexible and essentially tubular tether sub-spans. In the discretised non-planar tether model, environmental effects such as solar radiation, residual aerodynamic drag in low Earth orbit and electrodynamic forces, that may also influence the modelling, are reasonably assumed to be negligible in this context. The motor consists of a central rotor, which is attached to the propulsion tethers, and a stator which locates the rotor by means of a suitable bearing. The power supplies, control systems, and communication equipment are assumed to be fitted within the surrounding stator assembly in a practical installation. The stator also provides the necessary reaction that is required for the rotor to spin-up in a friction free environment. The motor torque acts about the motor drive axis, and it is assumed here that the motor drive axis will stay normal to the spin

plane of the propulsive tethers and payloads.

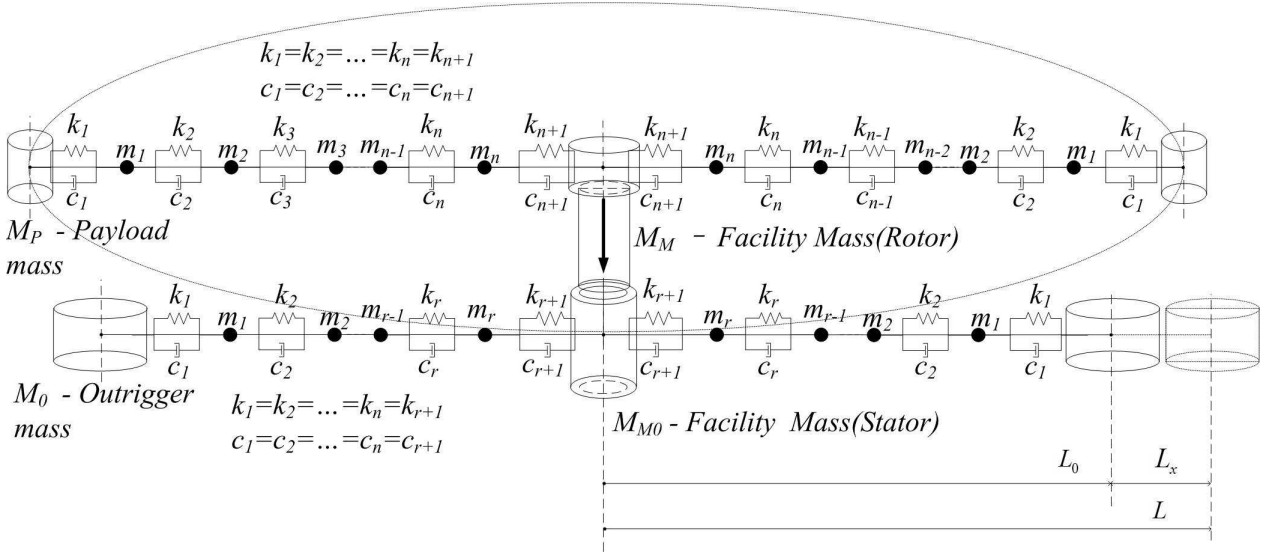


Figure 3: Modelling of Axial Elasticity for Motorised Momentum Exchange Tether [3]

The elasticity of the tether system is considered to be distributed symmetrically along each tether sub-span. The tether and the motor are connected by discrete spring-damper groups as shown in Figure 3. When the tether moves out of the orbital plane, the motor drive axis remains orthogonal to the spin plane, meanwhile, the motor torque will act about the principal axis through its centre of mass. The length of the discretised MMET from payload to COM, where the time variant length $L(t)$ of the tether is the sum of L_0 and $L_x(t)$, the static length and the variable elastic length of the discretised tether, respectively. There are six generalised coordinates in this model, in the form of four rotational coordinates $(\psi, \theta, \alpha, \gamma)$ and two translational coordinates $(L_x(t), R)$. Coordinate ψ defines the spin-up performance of the MMET system and is the ‘in-plane pitch angle’. This denotes the angle from the x_0 axis in Figure 2 to the projection of the tether onto the orbit plane. θ is the circular orbit angular position, effectively the true anomaly. α is an out-of-plane angle, from the projection of the tether onto the orbit plane to the tether, and is always within a plane normal to the orbit plane. γ defines rolling, and lies between the torque-plane and the tether-spin-plane. R is the distance from the Earth to the MMET COM, and L_x is the axial elastic length. Lagrange’s equations are used to obtain the dynamical equations of motion based on the six generalised coordinates [3].

3 Hybrid Control Strategy

To make the necessary enhancement required to obtain the F α SMC method, a hybrid control law is introduced. This combines the fuzzy logic control with sliding mode control in which a sliding hyperplane surface is generated by use of a skyhook damping law. Meanwhile, because the chattering phenomenon is an acknowledged drawback of sliding mode control and is usually caused by unmodelled system dynamics, a special boundary layer is proposed around the sliding surface is also taken to solve the chattering problem [15].

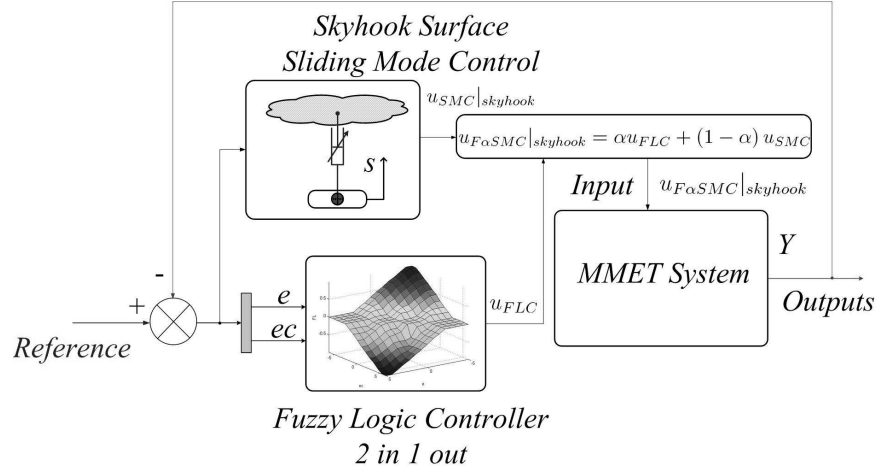


Figure 4: $F\alpha$ SMC flow diagram

A flow diagram for the $F\alpha$ SMC, and applying the SkyhookSMC approach, is given in Figure 4. The hybrid control effects of the FLC and the SkyhookSMC are combined by equation (1). In equation (1), α is a switching factor which balances the weight of the fuzzy logic control to that of the skyhook surface sliding mode control. Clearly, $\alpha = 0$ represents for SkyhookSMC, and $\alpha = 1$ represents for FLC, $\alpha \in [0,1]$.

$$u_{F\alpha SM C|skyhook} = \alpha u_{FLC} + (1 - \alpha) u_{SM C|skyhook} \quad (1)$$

3.1 Fuzzy Logic Controller Design

Fuzzy control is a practical alternative for a variety of challenging control applications since it provides a convenient method for constructing nonlinear controllers via the use of heuristic information. This may come from an operator that acts as a human-in-the-loop controller and from whom experiential data is obtained. The structure of the FLC for the the MMET system is shown in Figure 5. An ‘If-Then’ rule-base is then applied to describe the expert knowledge. The FLC rule-base is characterised by a set of linguistic description rules based on conceptual expertise which arises from typical human situational experience. Table 1 is the 2-in-1-out FLC rule-base table which can drive the FLC inference mechanism, and this came from previous experience gained from examining dynamic simulations for tether length changes during angular velocity control. Briefly, the main linguistic control rules are: (1) when the angular velocity decreases, the length tether increases; Conversely, when the angular velocity increases, the tether length decreases. (2) When the angular acceleration increases, the tether length increases can reduce the error between the velocity and the reference velocity; otherwise, when the angular acceleration decreases, the tether length decreases as well. A membership function (MF) is a curve that defines how each point in the input space is mapped to a membership value between 0 and 1. The MF for the MMET 6-DOF system is a Gaussian combination membership function. The inputs e and ec are interpreted from this fuzzy set, and the appropriate degree of membership is obtained [14].

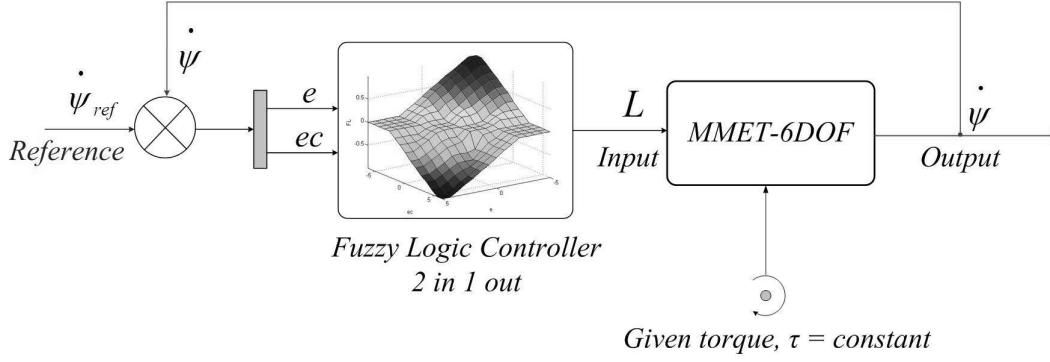


Figure 5: FLC flow diagram

Table 1: 2-in-1-out FLC rule table for MMET 6-DOF

U	EC								
	NB	NM	NS	NZS	ZE	PZS	PS	PM	PB
NB	NB	NM	NS	NZS	PZS	PZS	PS	PM	PB
NM	NM	NM	NZS	NZS	PZS	PZS	PZS	PM	PM
NS	NS	NS	NZS	NZS	PZS	PZS	PZS	PS	PS
NZS	NZS	NZS	NZS	NZS	ZE	PZS	PZS	PZS	PZS
E ZE	PZS	PZS	PZS	PZS	ZE	ZE	ZE	PZS	PZS
PZS	PZS	PZS	PZS	PZS	ZE	NZS	NZS	NZS	NZS
PS	PS	PS	PZS	PZS	PZS	NZS	NZS	NS	NS
PM	PM	PM	PS	PZS	PZS	NZS	NS	NM	NM
PB	PB	PM	PS	PZS	PZS	NZS	NS	NM	NB

3.2 Sliding Mode Control with Skyhook Surface Design

The objective of the SkyhookSMC controller is to consider the nonlinear tether system as the controlled plant, and therefore defined by the general state-space in equation (2):

$$\dot{x} = f(x, u, t) \quad (2)$$

where $x \in \mathbb{R}^n$ is the state vector, n is the order of the nonlinear system, and $u \in \mathbb{R}^m$ is the input vector, m is the number of inputs. $s(e, t)$ is the sliding surface of the hyperplane, which is given in equation (3) and shown in Figure 6, where λ is a positive constant that defines the slope of the sliding surface.

$$s(e, t) = \left(\frac{d}{dt} + \lambda \right)^{n-1} e \quad (3)$$

where λ is a positive constant that defines the slope of the sliding surface. The MMET system is a second-order system, so by letting $n = 2$, one obtains a second-order system in which s defines the position error (e) and velocity error (\dot{e}) in equation (4).

$$s = \dot{e} + \lambda e \quad (4)$$

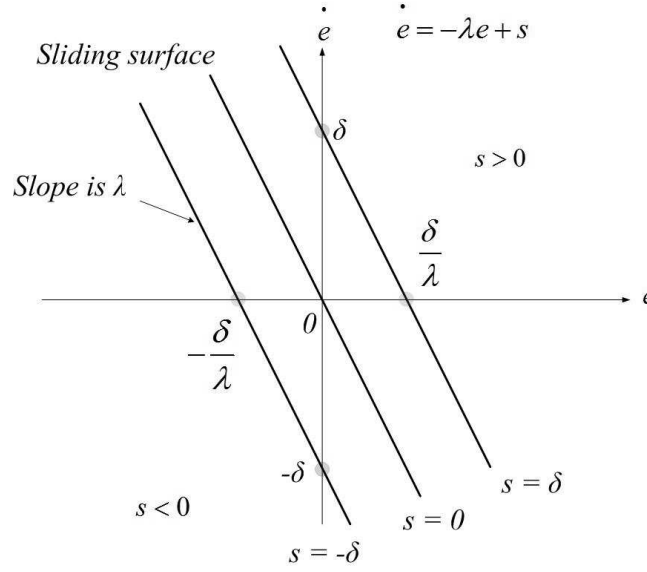


Figure 6: Sliding surface

From equations (3) and (4), the second-order tracking problem is now replaced by a first-order stabilization problem in which the scalar s is kept at zero by means of a governing condition. This is obtained from use of the Lyapunov stability theorem, given in equation (5), and it states that the origin is a globally asymptotically stable equilibrium point for the control system. Equation (5) is positive definite and its time derivative is given in inequality (6), to satisfy the negative definite condition, that the system should satisfy the inequality in (6).

$$V(s) = \frac{1}{2}s^2 \quad (5)$$

$$\dot{V}(s) = s\dot{s} < 0 \quad (6)$$

Skyhook control strategy was introduced in 1974 by Karnopp et al [16]. In Figure 7 the basic idea is to link a vehicle body's sprung mass to the the 'stationary sky' by a controllable 'skyhook' damper, which can then reduce vertical vibrations due to all kinds of road disturbance. Skyhook control can reduce the resonant peak of the sprung mass quite significantly and thus achieves a good ride quality in the car problem. By borrowing this idea to reduce the sliding chattering phenomenon, in Figure 8, a soft switching control law is introduced for the major sliding surface switching activity in equation (7), in order to reduce the chattering and to achieve good switch quality for the F α SMC combined with SkyhookSMC.

$$u_{SMC|skyhook} = \begin{cases} -c_0 \tanh\left(\frac{s}{\delta}\right) & s\dot{s} > 0 \\ 0 & s\dot{s} \leq 0 \end{cases} \quad (7)$$

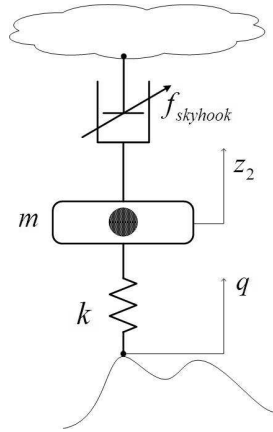


Figure 7: Ideal skyhook damper

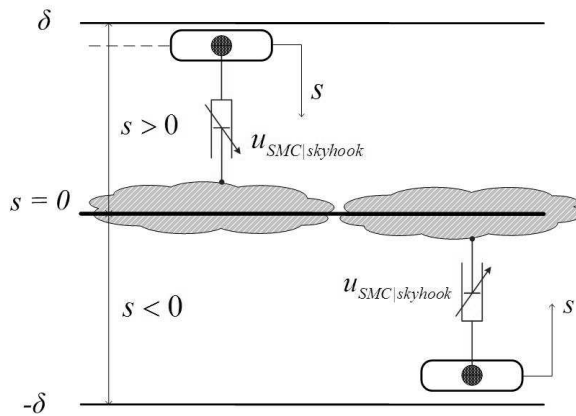


Figure 8: Sliding skyhook surface

where c_0 is an assumed positive damping ratio for the switching control law. This law needs to be chosen in such a way that the existence and the reachability of the sliding-mode are both guaranteed. Noting that δ is an assumed positive constant which defines the thickness of the sliding mode boundary layer [15].

4 Simulation and Conclusion

Numerical results are obtained using a specially devised co-simulation toolkit of MATLAB and MATHEMATICA functions in an integrated programme to provide a new toolbox, known henceforth here as SMATLINK. This integrates the control in MATLAB/SIMULINK and the MMET modelling in MATHEMATICA. The velocity and acceleration of ψ are selected as error (e) and change-in-error (ec) feedback signals for the the MMET system's spin-up control. Unless stated otherwise all the results are generated using the following parameters for the MMET 6-DOF system and controller in Table 2.

It is easy to switch the controller between the SkyhookSMC and the FLC modes when a proper value of α is selected ($0 < \alpha < 1$), and the hybrid fuzzy sliding mode controller is generated combining FLC with a soft continuous switching SkyhookSMC law based on

Table 2: MMET 6-DOF system parameters

N	number of mass points	20
μ	gravitational constant	$3.9877848 \times 10^{14} \text{ m}^3\text{s}^{-2}$
M_P	propulsion tether payload mass	1000 Kg
M_M	mass of motor facility	5000 Kg
r_{Tinner}	radius of tether inner tube	0.08 m
r_{Touter}	radius of tether outer tube	0.1 m
r_M	radius of motor facility	0.5 m
r_P	radius of payload	0.5 m
r_{per}	periapsis distance	$6.890 \times 10^6 \text{ m}$
r_{apo}	apoapsis distance	$1.0335 \times 10^7 \text{ m}$
L_0	static length tether sub-span	50000 m
A	undeformed tether tube cross-sectional area	$1.13097 \times 10^{-2} \text{ m}^2$
ρ	tether density	970 kg/m^3
e	orbit eccentricity	0.2
ψ_0	initial angular	0.0 rad
$\dot{\psi}_0$	initial angular velocity	0.0 rad/s
τ	motor torque	$2.5 \times 10^6 \text{ Nm}$
c_i	tether sub-span axial damping coefficient	$2 \times 10^6 \text{ Ns/m}$
k_i	tether sub-span axial stiffness	$2 \times 10^9 \text{ N/m}$
K_e	FLC scaling gains for e	1
K_{ec}	FLC scaling gains for ec	1
K_u	FLC scaling gains for u	21000
α	F α SMC switching factor	{0, 0.5, 1}
c_0	SkyhookSMC damping coefficient	-3000
δ	thickness of the sliding mode boundary layer	0.8
λ	slope of the sliding surface	0.0014

equation (7). All the control methods have an effect on the spin-up of the MMET 6-DOF system from the given initial conditions. The F α SMC hybrid fuzzy sliding mode control system parameters require a judicious choice of the FLC scaling gains of { K_e , K_{ec} } for fuzzification, K_u is the defuzzification gain factor which is used to map the control force to the range that actuators can generate practically. Similarly, the SkyhookSMC damping coefficient c_0 is required to expand the normalised controller output force into a practical range. The thickness of the sliding mode boundary layer is given by δ , and the slope of the sliding surface λ . Both data came from the previous MMET 6-DOF system spin-up simulation results without control, which are given in Table 2. In this simulation the F α SMC is used, with $\alpha = 0.5$ to balance the control weight between the FLC and the SkyhookSMC modes.

Different values of $\alpha = \{0.0, 0.5, 1.0\}$ can be used for {SkyhookSMC, F α SMC, FLC} control, respectively, for the MMET 6-DOF system. Figure 9 gives the time responses for the spin-up velocity $\dot{\psi}$, with different values of α , for the spin-up. These results show that all the control methods have an effect on the spin-up of the MMET system from the given initial conditions.

Figure 10 gives the axial elastic behaviour of the MMET in the simulation with the

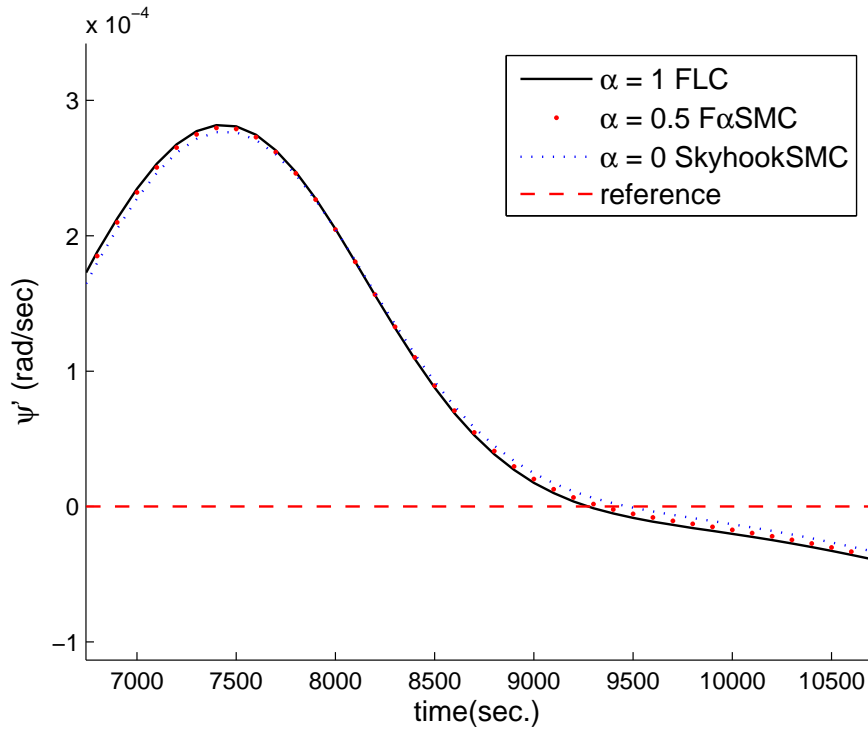


Figure 9: Spin-up velocity with different values of α

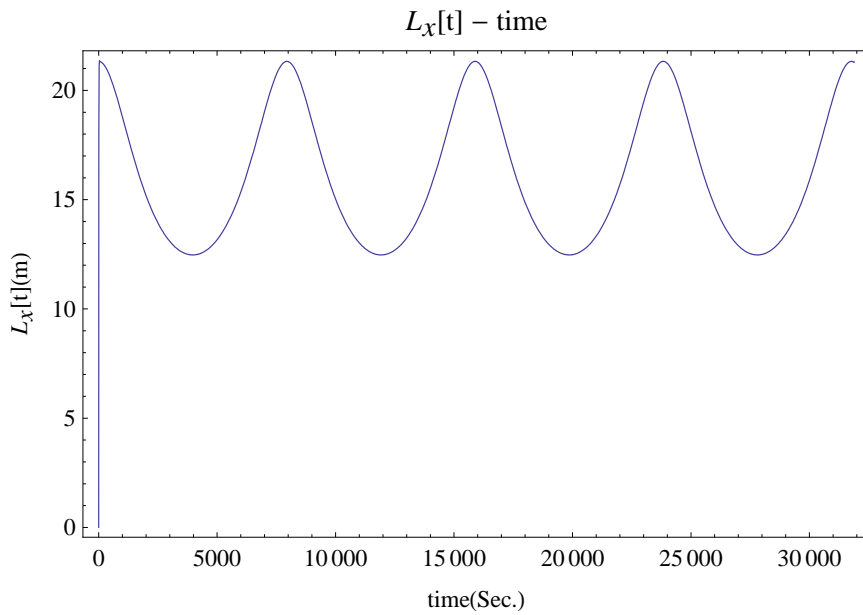


Figure 10: MMET axial elastic behaviour

appearance of stable axial oscillation.

The phase plane plots with different values of α are shown in Figure 11 as limit cycles whose behaviour for the spin-up coordinate ψ clearly corroborates interpretations of steady-state.

In Figure 12, the MMET spin-up error phase plane plots with different α are given,

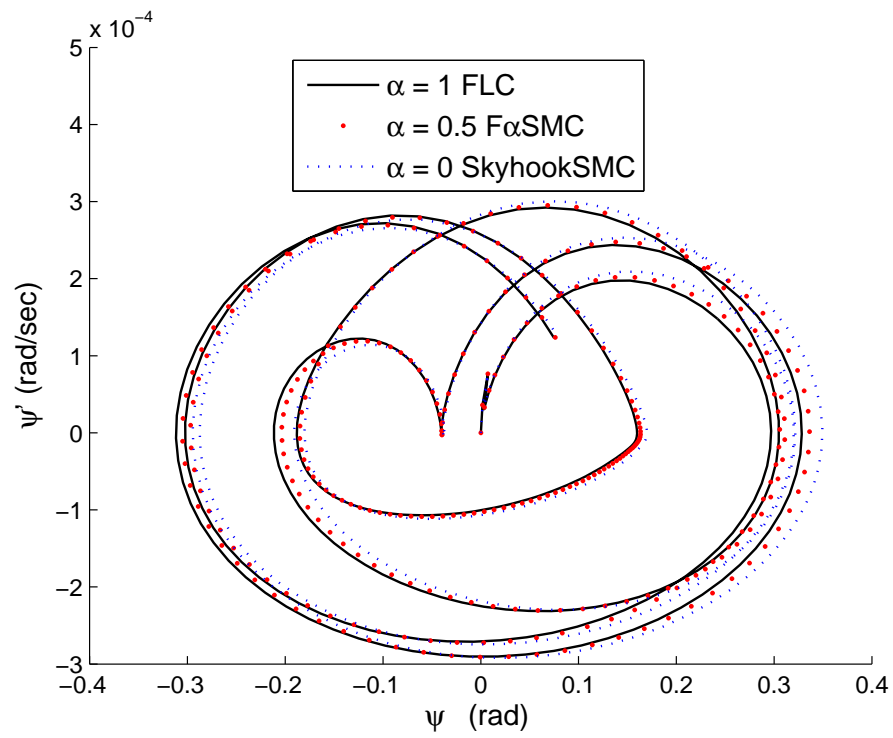


Figure 11: MMET spin-up phase plane plots with different values of α

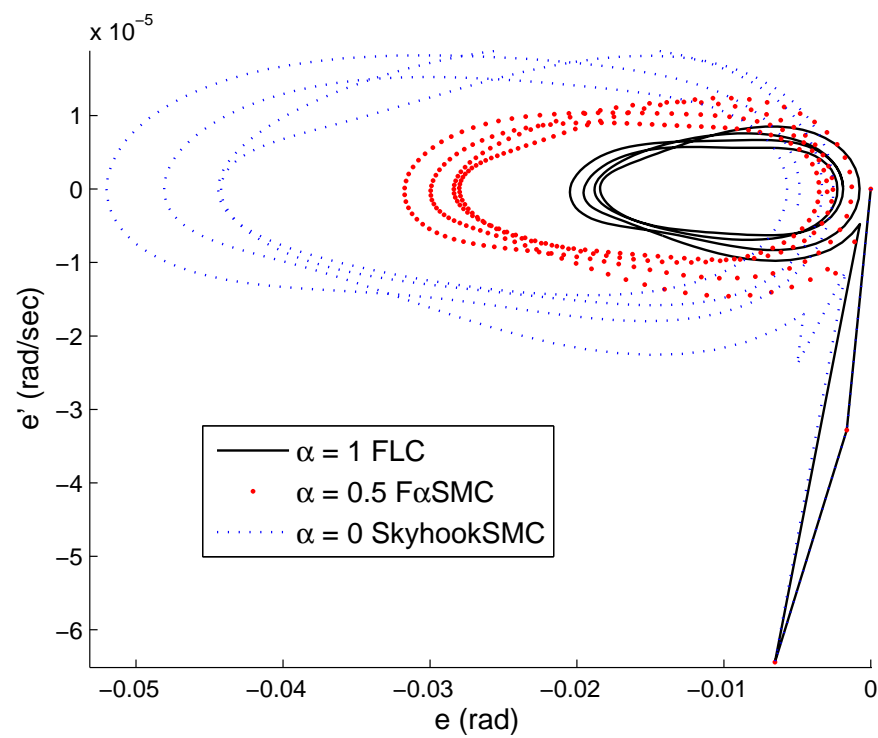


Figure 12: MMET spin-up errors phase plane plots with different values of α

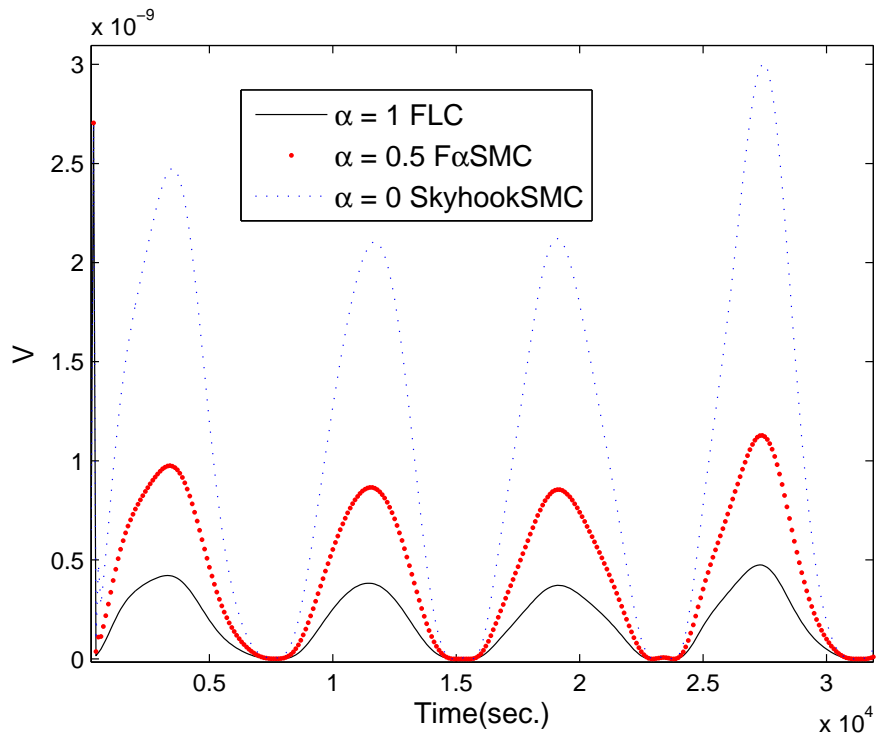


Figure 13: Lyapunov function for spin-up control methods with different α

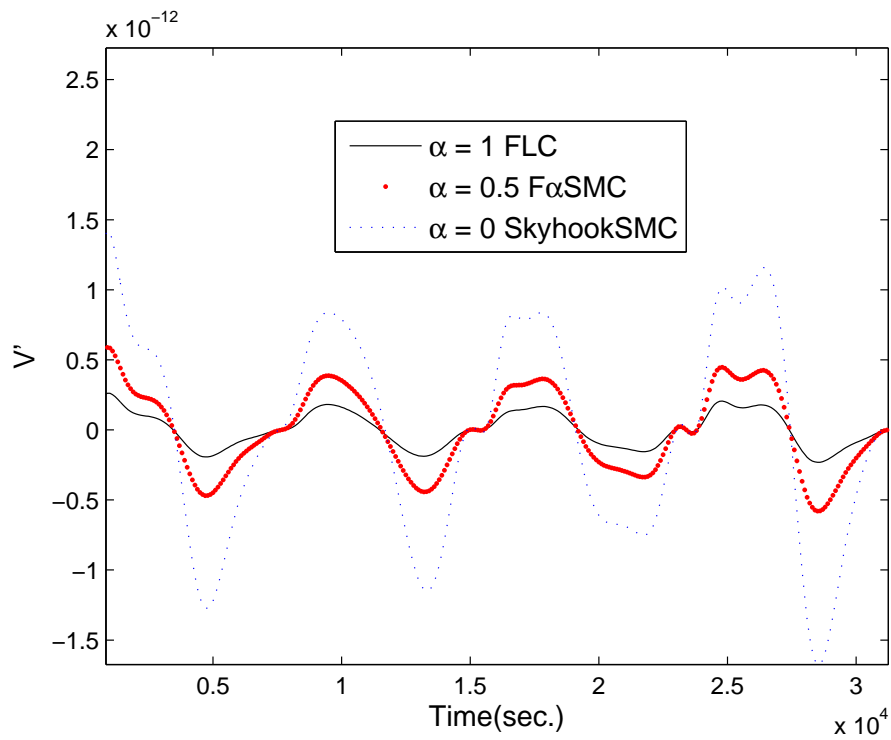


Figure 14: Sliding surface switching plot

and these shows that all the control methods offer limit cycles. The FLC caused generally faster response behaviour than the two other control methods for the spin-up coordinate ψ .

Figures 13 and 14 show the plots for the Lyapunov function and its derivative and this shows the effect of F α SMC control for different values of α . SkyhookSMC has higher energy activities than the two other control methods, and FLC has the lower associated energy around $V' = 0$, with the F α SMC's energy in the middle of the three. F α SMC can balance the control effects of FLC and SkyhookSMC for stable MMET 6-DOF spin-up outputs and associated energy activities.

5 Future work

The work in this paper has shown that by including the switching factor α , the F α SMC hybrid controller can switch and combine control from FLC to the SkyhookSMC rapidly, according to design requirements. This can balance the weight of the FLC and SkyhookSMC to override spin-up enhancement for the MMET 6-DOF system. The parameter settings for the F α SMC need further consideration because the current simulation results come from manual parameter tests. In order to enhance the parameter selection process and validation, some computational intelligence (CI) optimisation tools, such as Genetic Algorithms (GA) and Artificial Neural Networks (ANN), could be applied for parameter selection for the FLC, SMC and F α SMC. This would give some useful reference sets for parameter settings. A GA has already been used as an optimisation tool for parameter selection of the MMET system when applied to payload transfer from low Earth orbit (LEO) to geostationary Earth orbit (GEO), and the GA's optimisation ability has, in that case, been reasonably demonstrated [17].

Acknowledgements

The authors would like to acknowledge the support provided to the first author by the Overseas Research Students Awards Scheme and the Scholarship awarded by the University of Glasgow's Faculty of Engineering.

References

- [1] M. P. Cartmell, (1998), "Generating Velocity Increments by means of a Spinning Motorised Tether", 34th AIAA/ASME/SAE/ASEE Joint propulsion Conference and Exhibit, Cleveland Conference Centre, Cleveland, Ohio, USA, AIAA-98-3739.
- [2] S.W. Ziegler, and M. P. Cartmell, (2001), "Using Motorised Tethers for Payload Orbital Transfer", Journal of Spacecraft and Rockets, 38 (6), November / December, pp 904-913.
- [3] Y. Chen, M.P. Cartmell, (2007) "Dynamical Modelling of The Motorised Momentum Exchange Tether Incorporating Axial Elastic Effects", Advanced Problems in Mechanics , 20-28 June, Russian Academy of Sciences, St Petersburg, Russia.

- [4] Kevin M. Passino , Stephen Yurkovich, (1998), “Fuzzy Control”, Addison Wesley Longman, Menlo Park, CA.
- [5] S. V. Emelyanov, (1967), “Variable Structure Control Systems (in Russian)”, Moscow: Nauka.
- [6] Y. Itkis, (1976), “Control Systems of Variable Structure”, New York: Wiley
- [7] V. A. Utkin, (1978), “Sliding Modes and Their Application in Variable Structure Systems”, Moscow: Nauka (in Russian) (also Moscow: Mir, 1978, in English)
- [8] J.J.E. Slotine, and W.P. Li, (1991), “Applied Nonlinear Control”, Prentice-Hall International.
- [9] K. C. Ng, Y. Li, D. J. Murray-smith, K. C. Sharman, (1995), “Genetic Algorithm applied to Fuzzy Sliding Mode Controller design”, First International Conference on Genetic Algorithms in Engineering Systems: Innovations and Applications, GALE-SIA, 12-14 Sep 1995 Page(s):220 - 225.
- [10] Brian O’Dell, (1997), “Fuzzy Sliding Mode Control: A Critical Review”, Oklahoma State University, Advanced Control Laboratory, Technical Report ACL-97-001.
- [11] S. G. Tzafestas1 ,G. G. Rigatos1, (1999), “A Simple Robust Sliding-Mode Fuzzy-Logic Controller of the Diagonal Type”, Journal of Intelligent and Robotic Systems, Volume 26, Numbers 3-4 , pp 353-388.
- [12] E.H. Mamdani, (1977), “Applications of fuzzy logic to approximate reasoning using linguistic synthesis”, IEEE Transactions on Computers, Vol.26, No. 12, pp. 1182-1191.
- [13] I. Eksin, M. Güzelkaya, S. Tokat, (2002), “Self-Tuning Mechanism for Sliding Surface Slope Adjustment In Fuzzy Sliding Mode Controllers”, Proceedings of the Institution of Mechanical Engineers, Part I: Journal of Systems and Control Engineering, Volume 216, Number 5, Page 393-406.
- [14] Y. Chen, M.P. Cartmell, (2009), “Hybrid fuzzy and sliding-mode control for motorised tether spin-up when coupled with axial vibration”, 7th International Conference on Modern Practice in Stress and Vibration Analysis, 8-10 September 2009, New Hall, Cambridge, UK.
- [15] J.J. E. Slotine, (1982), “Tracking control of nonlinear systems using sliding surfaces with application to robot manipulations”, PhD Dissertation, Laboratory for Information and Decision Systems, Massachusetts Institute of Technology.
- [16] D. C. Karnopp, M. J. Crosby , R. A. Harwood, (1974), “Vibration Control Using Semi-Active Force Generators”, Journals of Engineering for Industry, Transactions of the ASME, 94:619-626.
- [17] Y. Chen, M.P. Cartmell, (2007), ”Multi-objective optimisation on motorised momentum exchange tether for payload orbital transfer”, IEEE Congress on Evolutionary Computation, Publication Date: 25-28 Sept. 2007, pp. 987-993.

* PhD student ** Professor

Department of Mechanical Engineering, University of Glasgow, Glasgow, G12 8QQ,
Scotland, UK.